Solid Earth Discuss., https://doi.org/10.5194/se-2017-103
Manuscript under review for journal Solid Earth
Discussion started: 27 September 2017

Effect of chemical composition on the electrical conductivity of gneiss at high temperatures and pressures

Lidong Dai[1,*], Wenqing Sun[1,2], Heping Li[1], Haiying Hu[1], Lei Wu[1], and Jianjun Jiang[1,2]

[1]Key Laboratory of High-Temperature and High-Pressure Study of the Earth's Interior, Institute of Geochemistry, Chinese Academy of Sciences, Guiyang, 550081, China

[2]University of Chinese Academy of Sciences, Beijing, 100049, China

Correspondence to: Lidong Dai (dailidong@vip.gyig.ac.cn)

Abstract. Electrical conductivities of the gneiss samples with different chemical compositions [W_A=Na_2O+K_2O+CaO=7.12%, 7.27% and 7.64% in weight percent] were measured using a complex impedance spectroscopic technique at 623–1073 K and 1.5 GPa in the frequency range of 10^{-1} to 10^6 Hz. In addition, conductivities of gneiss with W_A=7.12% were measured at 623–1073 K and 0.5–2.0 GPa. The results indicated that the conductivities of gneiss markedly increase with the increase of the total content of alkali and calcium ions. The conductivity of gneiss and temperature conform to an Arrhenius relation at a certain temperature range. The influence of pressure on conductivity of gneiss is weaker than that of temperature, and the conductivity increases with the increasing pressure. According to the various ranges of activation enthalpy (0.35–0.52 eV and 0.76–0.87 eV) corresponding to higher and lower temperature regions at 1.5 GPa, two main conduction mechanisms were suggested to dominate the conductivity of gneiss: impurity conduction in the lower temperature region and ionic conduction (charge carriers are K^+, Na^+ and Ca^{2+}) in the higher temperature region. Finally, it was confirmed that gneisses with various chemical compositions can't cause the high conductivity layers (HCLs) in Dabie-Sulu ultrahigh-pressure metamorphic belt.

Solid Earth Discuss., https://doi.org/10.5194/se-2017-103
Manuscript under review for journal Solid Earth
Discussion started: 27 September 2017

1 Introduction

According to magnetotelluric (MT) and geomagnetic depth sounding (GDS) results, electrical conductivities of geological samples at high temperatures and pressures can be used to extrapolate the mineralogical composition and thermodynamic state in the earth's interior (Maumus et al., 2005; Manthilake et al., 2015; Li et al., 2016; Dai et al., 2016; Hu et al., 2017). High conductivity layers (HCLs) are widely distributed in the middle-lower crust and upper mantle, and the cause of HCLs located in different regions may be various (Xiao et al., 2007, 2011; Pape et al., 2015; Novella et al., 2017). Hence, it is significant to systematically study the electrical conductivities of minerals and rocks which are distributed in the deep earth. A series of electrical conductivities on the main minerals and rocks have been systemically researched by previous studies under conditions of high temperatures and pressures (Fuji-ta et al., 2007; Hu et al., 2011, 2014; Dai et al., 2012; Yang et al., 2012; Dai and Karato, 2014; Sun et al., 2017). However, electrical conductivities of most metamorphic rocks haven't been explored at high temperatures and pressures, and thus the interpretations for HCLs distributed to representative regional metamorphic belts are still not comprehensive.

Regional metamorphic belt is a complicated geological unit. The results of geophysical exploration indicated that lots of places with anomaly high electrical conductivity have been observed in the metamorphic belts (Xiao et al., 2007; Wannamaker et al., 2009; Zeng et al., 2015). Metamorphic rocks (e.g., slate, schist, gneiss, granulite and eclogite) with different degrees of metamorphism play an important rule due to their widespread distribution in regional metamorphic belts. Dai et al. (2016) studied the electrical conductivity of dry eclogite at 873–1173 K, 1.0–3.0 GPa and various oxygen fugacity (solid oxygen buffers are Cu + CuO, Ni + NiO and Mo + MoO_2), and found that the hopping of small polaron is the dominant conduction mechanism for dry eclogite at high temperatures and pressures. The electrical conductivity of the natural eclogite is much lower than the conductivity of HCL in the

Dabie-Sulu ultrahigh-pressure metamorphic belt of eastern China. Granulite is another one important metamorphic rock which was distributed to most regional metamorphic belts. The conductivities of granulite are generally lowered by repeating the heating cycles, and the conductivity range is about 10^{-7}–10^{-2} S/m in the steady state of granulite at 1.0 GPa and up to about 900 K. Because of the complicated mineralogical assemblage and rock structure of granulite, the features of the electrical conductivity values in the heating cycles were not explained, and the conduction mechanism for granulite was not definitely stated (Fuji-ta et al., 2004). Gneiss is formed at mid- to lower crustal pressure–temperature conditions, and widely distributed in regional metamorphic belt. The main rock-forming minerals of gneiss are feldspar, quartz and biotite. Electrical conductivity of gneiss increases with the increase of temperature, and the conductivity range is about 10^{-4}–10^{-2} S/m at up to 1000 K and 1.0 GPa (Fuji-ta et al., 2007). Based on various chemical compositions and mineralogical constituents, gneisses are divided into different types. Therefore, it is crucial to investigate the electrical conductivity of gneisses with various chemical compositions and mineral constituents. Gneiss can be formed by the metamorphism of granite, and the mineralogical assemblage of gneiss is similar to that of granite. The electrical conductivity of granite dramatically increases with the increasing content of alkaline ions and calcium ions at 623–1173 K and 0.5–1.5 GPa. Impurity conduction was proposed to be the dominant conduction mechanism for granite in the lower-temperature region, and the alkane ions including K^+, Na^+ and Ca^{2+} were the probable charge carriers at higher temperatures (Dai et al., 2014).

In the present studies, we in-situ measured the electrical conductivities of the gneiss samples with various chemical compositions under the conditions of 0.5–2.0 GPa and 623–1073 K. According to the experimental results, we researched the dependence of temperature, pressure and chemical compositions on the electrical conductivity of gneiss. Based on the thermodynamic parameters and the relationship between electrical conductivity and chemical compositions, the conduction mechanisms were discussed in detail. Furthermore, we have explored the geophysical implication of the electrical conductivity for gneiss.

2 Experimental procedures

2.1 Sample preparation

Four fresh natural gneiss samples were collected from Xinjiang, China. In order to determine the mineralogical assemblage of gneiss, we applied optical microscopy and scanning electron microscopy (SEM) at the State Key Laboratory of Ore Deposit Geochemistry, Institute of Geochemistry, Chinese Academy of Sciences (CAS), Guiyang, China. The major element contents of the gneiss samples were analyzed by the X-ray fluorescence spectrometer (XRF) at Australian Laboratory Services (ALS), Shanghai, China. As shown in Fig. 1, the main rock-forming minerals of four gneiss samples are feldspar, quartz and biotite. The volume ratios of the same rock-forming mineral in different gneiss samples were various (Table 1). Table 2 showed the chemical compositions of whole rock analysis for the gneiss samples. Although the four gneiss samples had the same element types, the element content of the different samples were various.

2.2 Impedance measurements

High temperatures and pressures for the experiments were generated in the YJ-3000t multi-anvil apparatus, and the impedance spectra were collected using the Solartron-1260 Impedance/Gain-phase analyzer at the Key Laboratory of High-Temperature and High-Pressure Study of the Earth's Interior, Institute of Geochemistry, Chinese Academy of Sciences, Guiyang, China. All components of the experimental assemblage (ceramic tubes, pyrophyllite, and Al_2O_3 and MgO sleeves) were previously baked at 1073 K for 12 h in a muffle furnace to avoid the influence of absorbed water on the electrical conductivity measurements. As shown in Fig. 2, the sample was loaded into the magnesia tube. Two nickel disks (6.0 mm in diameter and

0.5 mm in thickness) on the top and bottom of sample were applied to be the electrodes. In order to shield against the external electromagnetic and spurious signal interference, a layer of nickel foil with the thickness of 0.025 mm was installed between the alumina and magnesia sleeve. Alumina and magnesia sleeve have good properties of insulating current and transmitting pressure. Pyrophyllite cube (edge length: 32.5 mm) was applied to be the pressure medium, and heater was composed of three-layer stainless steel sheets whose total thickness was 0.5 mm. The sample assembly was placed in an oven with a temperature of 330 K to keep it dry before experiment.

In the experiments, pressure was slowly increased to the desired value with a speed of 1.0 GPa/h, and then the temperature was increased at the rate of 300 K/h to the designated values. A Solartron-1260 Impedance/Gain-phase analyzer with an applied voltage of 3 V and the frequency range of 10^{-1}–10^{6} Hz was used to collect impedance spectra of samples when the pressure and temperature were stable. At the desired pressure, the spectra were measured at a certain temperature which was changed in 50 K intervals. The impedance spectra of gneiss samples with W_A (Na_2O+K_2O+CaO) = 7.12% were collected under conditions of 0.5–2.0 GPa and 623–1073 K. The spectra of other two gneiss samples with W_A= 7.27% and 7.64%, were measured at 623–1073 K and 1.5 GPa. In order to confirm the reproducibility of data, it was performed to measure the electrical conductivity of gneiss in two heating and cooling cycles at a constant pressure. The errors of temperatures and pressures were ±5 K and ±0.1 GPa, respectively.

3 Results

Typical complex impedance spectra were shown in Fig. 3. It was shown that all spectra were composed of an almost ideal semicircle in the high-frequency domain and an additional tail in the lower frequency domain. Other impedance spectra of the gneiss samples at different temperatures and pressures had the same characteristics of

Solid Earth Discuss., https://doi.org/10.5194/se-2017-103
Manuscript under review for journal Solid Earth
Discussion started: 27 September 2017

those shown in Fig. 3. Roberts and Tyburczy (1991) and Saltas et al. (2013) have suggested that the ideal semicircle represents the bulk electrical properties of the sample, and the additional tail is the usual characteristic of diffusion processes at the sample-electrode interface. Hence, the bulk sample resistance can be obtained by fitting the ideal semicircle in the high-frequency domain. A series connection of R_S-C_S (R_S and C_S represent the resistance and constant-phase element of the sample, respectively) and R_E-C_E (R_E and C_E represent interaction of charge carrier with electrode) was applied to be the equivalent circuit. All fitting errors of the electrical resistance were less than 5%. Based on the sample size and electrical resistance, the electrical conductivity of the sample was calculated by the following formula:

$$\sigma = L / SR, \tag{1}$$

where L is the height of the sample (m), S is the cross-sectional area of the electrodes (m^2), R is the fitting resistance (Ω) and σ is the electrical conductivity of the sample (S/m).

The logarithmic electrical conductivities of the gneiss samples were plotted against the reciprocal temperatures under conditions of 623–1073 K and 0.5–2.0 GPa. As shown in Fig. 4, the electrical conductivities of the gneiss with X_A = 7.12% were measured in two sequent heating and cooling cycles at 1.5 GPa. After the first heating cycle, electrical conductivities of the gneiss sample at the same temperature were close to each other in other cycles. It was confirmed that our experimental data were reproducible, and the gneiss sample has been kept a steady state after the first heating cycle. Two different linear relations of logarithmic electrical conductivity and reciprocal temperature were separated by an inflection point. Electrical conductivity of gneiss sample with W_A= 7.12% significantly increases with increasing temperature after 723 K at 0.5–1.0 GPa, and this phenomenon occurs after 773 K at 1.5–2.5 GPa (Fig. 5). As shown in Fig. 6, the electrical conductivities of the samples increased with increasing pressure, and the effect of pressure on conductivity was weaker than that of temperature. For other gneiss samples with W_A= 7.27% and 7.64%, the inflection points appears at 773 K under all designated pressures (Fig. 6). In a certain temperature range, the relationship between electrical conductivity and temperature

Solid Earth Discuss., https://doi.org/10.5194/se-2017-103
Manuscript under review for journal Solid Earth
Discussion started: 27 September 2017

fits the Arrhenius formula:

$$\sigma = \sigma_0 \exp(-\Delta H / kT), \quad (2)$$

where σ_0 is the pre-exponential factor (K S/m), k is the Boltzmann constant (eV/K), T is the absolute temperature (K), and ΔH is the activation enthalpy (eV). All fitting parameters for the electrical conductivities of four gneiss samples were listed in Table 3. The activation enthalpies for the gneiss samples are 0.35–0.58 eV at lower temperature range, and 0.71–1.05 eV at lower temperature range. In addition, the logarithms of pre-exponential factors were negative at lower temperature, but the values were positive at higher temperature range.

The total alkaline ion content of K_2O, Na_2O and CaO is a remarkable influence factor on the electrical conductivities of the gneiss samples. As shown in Fig. 6, the electrical conductivities of the gneiss samples increase with increasing total weight percent of K_2O, Na_2O and CaO. It reflected that the electrical conductivity of the gneiss samples was controlled mainly by minerals which contain abundant K_2O, Na_2O and CaO. The cations of feldspar are K^+, Na^+ and Ca^{2+}, and K^+ is also the main cation of biotite. Furthermore, impurity ions (K^+, Na^+ and Al^{3+}) were suggested to be the charge carriers for the quartz samples (Wang et al., 2010). Therefore, we can't distinguish which specific mineral is dominant to control the electrical conductivity of the gneiss samples. However, it was rational to consider the gneiss sample as a complex whole, and analyze the electrical conductivity of the gneiss samples with various chemical compositions at high temperatures and pressures.

4 Discussions

4.1 Comparisons with previous studies

As three constituent minerals of gneiss, feldspar, biotite and quartz dominated the electrical conductivities of rock at high temperatures and pressures. Due to the sophisticated mineralogical assemblage and rock structure, the gneiss samples were unstable in the first heating cycle. In this process, the impurity ions may be distributed, the grain size was slightly changed and the microcracks were gradually closed. After the first cycle, the electrical conductivity of gneiss sample has a good repeatability. It inflected that the gneiss sample has been in a stable state. The electrical conductivity range of gneiss samples with various chemical compositions is about 10^{-5}–10^{-1} S/m at 623–973 K and 0.5–2.0 GPa. The electrical conductivity of gneiss was slightly related to pressure, and it conforms to the previous conclusion that the influence of pressure on the conductivities of minerals and rocks is much weaker than that of temperature (Xu et al., 2000; Hu et al., 2011). The possible reason is that the effect of pressure on the activity of the charge carriers is weaker than that of temperature. The total alkaline ion content of K_2O, Na_2O and CaO is one crucial influence ingredient on the electrical conductivity of gneiss. Previous studies have researched the electrical conductivity of minerals and rocks with various chemical compositions, and the conclusions were similar to ours (Dai et al., 2014). Fiji-ta et al. (2007) has studied the electrical conductivity of gneiss perpendicular and parallel to foliation at up to 1000 K and a constant pressure of 1.0 GPa. The conductivity of gneiss measured perpendicular to foliation was one magnitude lower than the value measured parallel to foliation. However, the influences of pressure and chemical compositions on the electrical conductivities of gneisses weren't been researched. In this study, we researched the electrical conductivity of gneiss parallel to foliation. As shown in Fig. 7, the electrical conductivity of gneiss of Fuji-ta et al. (2007) were higher than our results in the lower temperature range, whereas the values were lower than the conductivities of gneisses with W_A= 7.27% and 7.64% in this study. The discrepancy is probably caused by the various chemical compositions of the gneiss samples. Dai et al. (2014) measured the electrical conductivity of granite at 0.5–1.5 GPa and 623–1173 K, and the main rock-forming minerals are also quartz, feldspar, and biotite. It was found that the content of calcium and alkali ions significantly influences the electrical conductivities of gneiss. Electrical conductivities of granite and gneiss increase with increasing content of calcium and alkali ions. However, the electrical conductivities of granite were much lower than those of gneiss (Fig. 7). The discrepancy may be caused by the various chemical compositions and rock structure of granite and gneiss. Feldspars are important rock-forming minerals of gneiss, and thus it is important to compare the electrical conductivities of feldspars. The electrical conductivities of K-feldspar are one magnitude lower than the values of albite, and K^+ and Na^+ ions are the charge carriers of K-feldspar and albite, respectively (Hu et al., 2013). As shown in Fig. 7, the electrical conductivities of alkali feldspars are much higher than the values of the gneiss samples. It may be due to that the concentrations of alkali ions of alkali feldspars were higher than those of gneisses. In addition, granulite is another significant metamorphic rock, and usually coexists with gneiss. The electrical conductivities of granulite are moderately higher than the values of gneiss. The electrical conductivities of quartz at 1.0 GPa were slightly lower than the values of the gneiss with X_A = 7.27% at 1.5 GPa, and the slope of the linear relation between the logarithm of electrical conductivity and the reciprocal of temperature for quartz is close to that for gneiss at lower temperature range (Fuji-ta et al., 2004). The conductivities of phlogopite were higher than those of the gneiss with X_A = 7.64% at higher temperatures (above 773 K), and lower than those of the gneiss samples at lower temperatures (below 773 K). Furthermore, the slope of the linear relation between the logarithm of electrical conductivity for the phlogopite sample and the reciprocal of temperature is much higher than the slopes for the gneiss samples (Li et al., 2016).

4.2 Conduction mechanism

The logarithm of electrical conductivities and reciprocal temperatures conform to linear relation at higher and lower temperature range, respectively. This implies that the dominant conduction mechanism for our gneiss samples at lower temperature range is different from that at higher temperature range. The mineralogy assemblage and chemical compositions of gneiss samples are very complicated, and thus the conduction mechanisms for gneiss samples are difficult to be determined. Feldspars, quartz and biotite are dominant minerals of gneiss samples. Previous studies have suggested that the conduction mechanism for feldspar minerals is ionic conduction and the charge carriers are K^+, Na^+ and Ca^{2+} (Hu et al., 2013, 2015). The conduction mechanism for biotite hasn't been researched, whereas the charge carrier of phlogopite was proposed to be F^+ and K^+ (Li et al., 2016). For quartz, the conduction mechanism was impurity ionic conduction, and the dominant charge carriers are migrated by moving the alkali ions in channels (Wang et al., 2010). Therefore, we deduced that the conduction mechanism for gneiss samples may be related with ions. The activation enthalpy is an important evidence of the conduction mechanism for minerals and rocks (Dai et al., 2016). As Table 2 listed, the activation enthalpies for gneiss samples are 0.35–0.58 eV at lower temperature range, and 0.77–0.87 eV at higher temperature. Dai et al. (2014) studied the electrical conductivities of granite which has the same mineralogical assemblage with gneiss samples. It was proposed that the conduction mechanism at low temperatures was impurity conduction owing to low activation enthalpy (0.5 eV), whereas the mechanism is ionic conduction with high activation enthalpy (1.0 eV) at higher temperatures. The activation enthalpies for gneiss are close to the values for granite at lower and higher temperature ranges, respectively. On the other hand, the activation enthalpies for albite and K-feldspar were 0.84 and 0.99 eV, respectively (Hu et al., 2013). In addition, Fig. 4 shows that the increasing content of alkali and calcium ions significantly enhances the electrical conductivity of gneiss samples. Therefore, impurity conduction and ionic conduction were suggested to be the conduction mechanisms at lower and higher temperature range, respectively.

4.3 Effect of chemical compositions on electrical conductivity

The influence of chemical compositions (Na_2O+K_2O+CaO) on the electrical conductivity of the gneiss samples were very significant, as seen in studies concerning electrical conductivity of granite samples been closely related to the content of alkali and calcium ions (Dai et al., 2014). The electrical conductivities of granite samples at high temperatures and high pressures can be fitted as a function of

$(Na_2O+K_2O+CaO)/SiO_2$ (Dai et al., 2014). However, the electrical conductivity of gneiss samples doesn't regularly change with the variation of $(Na_2O+K_2O+CaO)/SiO_2$. The phenomenon shows that the dependence of electrical conductivity of gneiss on the chemical compositions is not identical to that of granite. This may be due to the more complicated mineralogical assemblage and chemical compositions of gneiss. Hu et al. (2013) has demonstrated that the electrical conductivity of alkali feldspar significantly depends on the value of Na/(Na+K). It inflects that the electrical conductivity of gneiss is not only affected by the total content of alkali and calcium ions, but also influenced by the ratios between various ions.

5 Geophysical implication

Abundant gneisses are distributed to Dabie-Sulu ultrahigh-pressure metamorphic belt, and the metamorphic conditions of gneiss correspond to the environments of mid- to lower crust (Wang et al., 2005; Liou et al., 2009; Zhang et al., 2009). Magnetotelluric (MT) and geomagnetic depth sounding (GDS) results have shown that a plenty of HCLs are distributed to Dabie-Sulu ultrahigh-pressure metamorphic belt. However, there was no clear interpretation for the HCLs. The electrical conductivities of natural eclogite and granulite were much lower than the conductivities for the HCLs (Fuji-ta et al., 2004; Dai et al., 2016). Therefore, it is significant to explore whether the electrical conductivity of gneiss can interpret the HCLs in the depth of the metamorphic belts. According to the typical heat flow value of the Dabie-Sulu terrane (75 mW/m^2) (He et al., 2009), the correspondent laboratory-based profiles can be constructed by converting the conductivity-temperature data into conductivity-depth results (Fig. 8). Because of minor influence of pressure on the electrical conductivity, and we ignored the electrical conductivities at other pressures. In order to compare with the conductivities of main metamorphic rocks, the conductivity-temperature data of eclogite (with three different controls on oxygen fugacity) and granulite were converted into conductivity-depth results using the same transformation method. As shown in Fig. 8, the electrical conductivities of HCL Dabie-Sulu terrane are $10^{-1.5}$–$10^{-0.5}$ S/m corresponding to 12–21 km. The high electrical conductivities were compared with the conductivities of three different rocks.

Although the electrical conductivities of gneiss were higher than the values of granulite and eclogite at the same depths, it was obvious that the electrical conductivities of granulite, eclogite and gneiss were all much lower than those of HCLs in the Dabie-Sulu terrane (Fig. 8). Therefore, The HCLs distributed in these regions are not caused by gneiss, eclogite or granulite. According to the previous studies, the electrical conductivity of hydrous fluid, partial melting, brine-bearing fluids, the interconnected secondary high conductivity phases (e.g., graphite, ilmenite, magnetite and pyrie etc. along the grain boundaries of minerals) and dehydration of minerals may cause the high conductivity anomalies in the deep crust (Duba et al., 1982; Frost et al., 1989; Hyndman et al., 1993; Maumus et al., 2005; Gaillard et al., 2008; Yang et al., 2011; Dai and Karato, 2014; Shimojuku et al., 2014; Manthilake et al., 2015, 2016; Hu et al., 2017). Although the electrical conductivity of the gneiss samples with different chemical compositions can't be used to interpret the HCLs, the conductivity-depth profiles we have constructed for gneiss with different chemical compositions may provide important constraints on the interpretation for field magnetotelluric conductivity in the regional metamorphic belts.

6 Conclusions

The electrical conductivity range of gneiss samples with various chemical compositions is about 10^{-5}–10^{-1} S/m at 623–973 K and 0.5–2.0 GPa. Electrical conductivities of the gneiss samples significantly increased with the increasing temperatures, and weakly increased with the increase of pressure. The total alkaline ion content of K_2O, Na_2O and CaO is a remarkable influence factor on the electrical conductivities of the gneiss samples. Based on the various activation enthalpy ranges (0.35–0.52 eV and 0.76–0.87 eV) corresponding to higher and lower temperature regions at 1.5 GPa, two main conduction mechanisms were suggested to dominate the conductivity of gneiss: impurity conduction in the lower temperature region and ionic conduction (charge carriers are K^+, Na^+ and Ca^{2+}) in the higher temperature region.

Due to the much lower conductivities of gneiss samples at high temperatures and pressures, it was confirmed that gneisses with various chemical compositions can't cause the high conductivity layers (HCLs) in Dabie-Sulu ultrahigh-pressure metamorphic belt.

Acknowledgements. This research was financially supported by the Strategic Priority Research Program (B) of the Chinese Academy of Sciences (XDB 18010401), Key Research Program of Frontier Sciences of CAS (QYZDB-SSW-DQC009), "135" Program of the Institute of Geochemistry of CAS, Hundred Talents Program of CAS and NSF of China (41474078, 41774099 and 41772042).

References

Dai, L.D. and Karato, S.: Influence of FeO and H on the electrical conductivity of olivine. Phys. Earth Planet. Inter., 237, 73–79, 2014.

Dai, L.D., Hu, H.Y., Li, H.P., Jiang, J.J., and Hui, K.S.: Influence of temperature, pressure, and chemical composition on the electrical conductivity of granite. Am. Mineral., 99, 1420–1428, 2014.

Dai, L.D., Hu, H.Y., Li, H.P., Wu, L., Hui, K.S., Jiang, J.J., and Sun, W.Q.: Influence of temperature, pressure, and oxygen fugacity on the electrical conductivity of dry eclogite, and geophysical implications. Geochem. Geophys. Geosyst., 17, 2394–2407, 2016.

Dai, L.D., Li, H.P., Hu, H.Y., Shan, S.M., Jiang, J.J., and Hui, K.S.: The effect of chemical composition and oxygen fugacity on the electrical conductivity of dry and hydrous garnet at high temperatures and pressures. Contrib. Mineral. Petrol., 163, 689–700, 2012.

Duba, A.G. and Shankland, T.J.: Free carbon and electrical conductivity in the Earth's mantle. Geophys. Res. Lett., 9, 1271–1274, doi: 10.1029/GL009i011p01271, 1982.

Frost, B.R., Fyfe, W.S., Tazaki, K., and Chan, T.: Grain-boundary graphite in rocks and implications for high electrical conductivity in the lower crust. Nature, 340, 134–136, 1989.

Fuji-ta, K., Katsura, T., and Tainosho, Y.: Electrical conductivity measurement of granulite under mid- to lower crustal pressure-temperature conditions. Geophys. J. Int., 157, 79–86, 2004.

Fuji-ta, K., Katsura, T., Matsuzaki, T., and Ichiki, M.: Electrical conductivity measurements of brucite under crustal pressure and temperature conditions. Earth Planets Space, 59, 645–648, 2007.

Fuji-ta, K., Katsura, T., Matsuzaki, T., Ichiki, M., and Kobayashi, T.: Electrical conductivity measurement of gneiss under mid- to lower crustal *P-T* conditions. Tectonophysics, 434, 93–101, 2007.

Gaillard, F., Malki, M., Iacono-Marziano, G., Pichavant, M., and Scaillet, B.: Carbonatite melts and electrical conductivity in the asthenosphere. Science, 322, 1363–1365, 2008.

He, L., Hu, S., Yang, W., and Wang, J.: Radiogenic heat production in the lithosphere of Sulu ultrahigh-pressure metamorphic belt. Earth Planet. Sci. Lett., 277, 525–538, 2009.

Hu, H.Y., Dai, L.D., Li, H.P., Hui, K.S., and Sun, W.Q.: Influence of dehydration on the electrical conductivity of epidote and implications for high conductivity anomalies in subduction zones. J. Geophys. Res., 122, 2751–2762, doi: 10.1002/2016JB013767 , 2017.

Hu, H.Y., Li, H.P., Dai, L.D., Shan, S.M., and Zhu, C.M.: Electrical conductivity of albite at high temperatures and high pressures. Am. Mineral., 96, 1821–1827, 2011.

Hu, H.Y., Li, H.P., Dai, L.D., Shan, S.M., and Zhu, C.M.: Electrical conductivity of alkali feldspar solid solutions at high temperatures and high pressures. Phys. Chem. Miner., 40, 51–62, 2013.

Hui, K.S., Dai, L.D., Li, H.P., Hu, H.Y., Jiang, J.J., Sun, W.Q., and Zhang, H.: Experimental study on the electrical conductivity of pyroxene andesite at high temperature and high pressure. Pure Appl. Geophys., 174, 1033–1041, 2017.

Hyndman R.D., Vanyan, L.L., and Marquis, G.: The origin of electrically conductive lower continental crust: saline water or graphite?. Phys. Earth Planet. Inter., 81: 325–344, 1993.

Li, Y., Yang, X.Z., Yu, J.H., and Cai, Y.F.: Unusually high electrical conductivity of phlogopite: the possible role of fluorine and geophysical implications. Contrib. Mineral. Petrol., 171, 37, 2016.

Liou, J.G., Ernst, W.G., Zhang, R.Y., Tsujimori, T., and Jahn, B.M.: Ultrahigh-pressure minerals and metamorphic terranes–The view from China. J. Asian Earth Sci., 35, 199–231, 2009.

Manthilake, G., Bolfan-Casanova, N., Novella, D., Mookherjee, M., and Andrault, D.: Dehydration of chlorite explains anomalously high electrical conductivity in the mantle wedges. Sci. Adv., 2, e1501631, 2016.

Manthilake, G., Mookherjee, M., Bolfan-Casanova, N., and Andrault, D.: Electrical conductivity of lawsonite and dehydrating fluids at high pressures and temperatures. Geophys. Res. Lett., 42, 7398–7405, doi: 10.1002/2015GL064804, 2015.

Maumus, J., Bagdassarov, N., and Schmeling, H.: Electrical conductivity and partial melting of mafic rocks under pressure. Geochim. Cosmochim. Acta., 69, 4703–4718, 2005.

Novella, D., Jacobsen, B., Weber, P.K., Tyburczy, J.A., Ryerson, F.J., and Du Frane, W.L.: Hydrogen self-diffusion in single crystal olivine and electrical conductivity of the earth’s mantle. Sci. Rep., 7, 5344, 2017.

Pape, L.P., Jones, A.G., Unsworth, M.J., Vozar, J., Wei, W.B., Jin, S., Ye, G.F., Jing, J.N., Dong, H., Zhang, L.T., and Xie, C.L.: Constraints on the evolution of crustal flow beneath Northern Tibet. Geochem. Geophys. Geosyst., 12, 4237–4260, 2015.

Roberts, J.J. and Tyburczy, J.A.: Frequency dependent electrical properties of polycrystalline olivine compacts. J. Geophys. Res., 96, 16205–16222, doi: 10.1029/91JB01574, 1991.

Saltas, V., Chatzistamou, V., Pentari, D., Paris, E., Triantis, D., Fitilis, I., and

Solid Earth Discuss., https://doi.org/10.5194/se-2017-103
Manuscript under review for journal Solid Earth
Discussion started: 27 September 2017

Vallianatos, F.: Complex electrical conductivity measurements of a KTB amphibolite sample at elevated temperatures. Mater. Chem. Phys., 139, 169–175, 2013.

Shimojuku, A., Yoshino, T., and Yamazaki, D.: Electrical conductivity of brine-bearing quartzite at 1 GPa: Implications for fluid content and salinity of the crust. Earth Planets Space, 66, 1–9, 2014.

Sun, W.Q., Dai, L.D., Li, H.P., Hu, H.Y., Wu, L., and Jiang, J.J.: Electrical conductivity of mudstone before and after dehydration at high temperatures and pressures. Am. Mineral., in press, doi: https://doi.org/10.2138/am-2017-6146, 2017.

Wang, D.J., Li, H.P., Matsuzaki, T., and Yoshino, T.: Anisotropy of synthetic quartz electrical conductivity at high pressure and temperature. J. Geophys. Res., 115, B09211, doi: 10.1029/2009JB006695, 2010.

Wang, Q., Ji, S.C., Salisbury, M.H., Xia, B., Pan, M.B., and Xu, Z.Q.: Pressure dependence and anisotropy of P-wave velocities in untrahigh-pressure metamorphic rocks from the Dabie-Sulu orogenic belt (China): Implications for seismic properties of subducted slabs and origin of mantle reflections. Tectonophysics, 398, 67–99, 2005.

Wannamaker, P.E., Caldwell, T.G., Jiracek, G.R., Maris, V., Hill, G.J., Ogawa, Y., Bibby, H.M., Bennie, S.L., and Heise, W.: Fluid and deformation regime of an advancing subduction system at Marlborough, New Zealand. Nature, 460, 733–736, 2009.

Xiao, Q.B., Cai, X.P., Liang, G.H., Xu, X.W., and Zhang, B.L.: Application of 2D magnetotelluric methods in a geological complex area, Xinjiang, China. J. Appl. Geophys., 75, 19–30, 2011.

Xiao, Q.B., Zhao, G.Z., Zhan, Y., Chen, X.B., Tang, J., Wang, J.J., and Deng, Q.H.: A preliminary study on electrical structure and dynamics of the ultra-high pressure metamorphic belt beneath the Dabie Mountains. Chinese J. Geophys., 50, 710–721, 2007.

Xu, Y.S., Shankland, T.J., and Duba, A.G.: Pressure effect on electrical conductivity of mantle olivine. Phys. Earth Planet. Inter., 118, 149–161, 2000.

Yang, X.Z., Keppler, H., McCammon, C., and Ni, H.W.: Electrical conductivity of orthopyroxene and plagioclase in the lower crust. Contrib. Mineral. Petrol., 163, 33–48, 2012.

Zeng, S.H., Hu, X.Y., Li, J.H., Xu, S., Fang, H., and Cai, J.C.: Detection of the deep crustal structure of the Qiangtang terrane using magnetotelluric imaging. Tectonophysics, 661, 180–189, 2015.

Zhang, R.Y., Liou, J.G., and Ernst, W.G.: The Dabie-Sulu continental collision zone: A comprehensive review. Gondwana Res., 16, 1–26, 2009.

Solid Earth Discuss., https://doi.org/10.5194/se-2017-103
Manuscript under review for journal Solid Earth
Discussion started: 27 September 2017

Figure captions

Fig. 1 Photomicrographs and electron backscattered images of four natural gneiss samples under the polarizing microscope. Pl=plagioclase; Qtz = quartz; Bt = Biotite.

Fig. 2 Experimental setup for electrical conductivity measurements at high temperatures and pressures.

Fig. 3 Representative complex impedance spectra of the gneiss samples at 1.5 GPa and 623–1073 K.

Fig. 4 Logarithm of the electrical conductivities versus the reciprocal temperatures of the gneiss sample during two heating/cooling cycles at 1.5 GPa.

Fig. 5 Logarithm of the electrical conductivities versus the reciprocal temperatures of the samples at 0.5–2.5 GPa and 623–1073 K.

Fig. 6 Logarithm of the electrical conductivities versus the reciprocal temperatures of the gneiss samples with various chemical compositions at 1.5 GPa and 623–1073 K.

Fig. 7 Comparisons of the electrical conductivities of the gneiss samples measured at 1.5 GPa in this study and in previous studies. The dashed blue and green lines represent the electrical conductivities of gneiss and granulite at 1.0 GPa from Fuji-ta et al. (2004) and Fuji-ta et al. (2007), respectively, the dashed violet line represents the electrical conductivity of quartz at 1.0 GPa from Wang et al. (2010), the dashed brown line represents the electrical conductivity of alkali feldspars at 1.0 GPa from Hu et al. (2013), the dashed red line represents the electrical conductivity of granite at 0.5 GPa from Dai et al. (2014), and the dashed pink line represents the electrical conductivity of phlogopite at 1.0 GPa from Li et al. (2016).

Fig. 8 Laboratory-based conductivity–depth profiles constructed from data of the gneiss samples, and the thermodynamic parameters, and comparison with geophysically inferred field results from Dabie-Sulu ultrahigh-pressure metamorphic belt, China. The red solid lines represent the conductivity–depth profiles based on the conductivities of the samples described in Fig. 3 and based

Solid Earth Discuss., https://doi.org/10.5194/se-2017-103
Manuscript under review for journal Solid Earth
Discussion started: 27 September 2017

on a surface heat flow of 75 mW/m^2 in Dabie-Sulu ultrahigh-pressure metamorphic belt. The dashed blue lines represent the conductivity–depth profiles based on the conductivities of eclogite, and the dashed brown line represents the conductivity–depth profiles based on the conductivities of granulite (Fuji-ta et al. 2004; Dai et al. 2016). The green region represents the magnetotelluric data derived from the high-conductivity layer in Dabie-Sulu ultrahigh-pressure metamorphic belt (Xiao et al. 2007; He et al. 2009).

Solid Earth Discuss., https://doi.org/10.5194/se-2017-103
Manuscript under review for journal Solid Earth
Discussion started: 27 September 2017

Table 1 mineralogical assemblage of three natural gneiss samples. Pl=plagioclase, Qz=quartz and Bi=Biotite.

No.	Mineral associations
DS12	Pl (50%) + Qz (40%) + Bi (10%)
DS13	Pl (25%) + Qz (40%) + Bi (35%)
DS14	Pl (60%) + Qz (25%) + Bi (15%)

Solid Earth Discuss., https://doi.org/10.5194/se-2017-103
Manuscript under review for journal Solid Earth
Discussion started: 27 September 2017

Table 2 Chemical compositions of X-ray fluorescence (XRF) analyses for three gneiss samples.

Oxides (wt.%)	DS12	DS13	DS14
SiO_2	64.40	68.59	69.87
Al_2O_3	15.30	13.62	14.88
MgO	3.15	3.00	1.78
CaO	1.61	2.48	0.52
Na_2O	2.27	2.46	2.26
K_2O	3.24	2.33	4.86
Fe_2O_3	6.28	5.57	3.37
TiO_2	0.81	0.61	0.38
Cr_2O_3	0.02	0.02	0.01
MnO	0.08	0.07	0.03
BaO	0.06	0.02	0.12
SrO	0.03	0.03	0.02
P_2O_5	0.19	0.16	0.08
SO_3	<0.01	<0.01	0.28
L.O.I	1.89	0.86	1.67
Total	99.33	99.82	100.13

Solid Earth Discuss., https://doi.org/10.5194/se-2017-103
Manuscript under review for journal Solid Earth
Discussion started: 27 September 2017

Solid Earth Discussions

Table 3 Fitted parameters of the Arrhenius relation for the electrical conductivity of three gneiss samples.

Run No.	*P* (GPa)	*T* (K)	Log σ_0 (S/m)	ΔH (eV)	γ^2
DS12	0.5	623-723	-0.20±0.09	0.58±0.01	99.91
		723-1073	1.11±0.08	0.77±0.01	99.79
	1.0	623-723	-0.06±0.01	0.56±0.01	99.99
		723-1073	0.98±0.08	0.72±0.01	99.77
	1.5	623-773	-0.06±0.02	0.52±0.02	99.66
		773-1073	1.43±0.05	0.76±0.01	99.93
	2.0	623-773	-0.38±0.05	0.47±0.01	99.96
		773-1073	1.26±0.11	0.71±0.03	99.51
DS13	1.5	623-773	-0.92±0.04	0.35±0.01	99.93
		773-1073	2.26±0.12	0.84±0.01	99.66
DS14	1.5	623-773	-0.49±0.10	0.38±0.01	99.60
		773-1073	2.63±0.10	0.87±0.02	99.81

Fig. 1

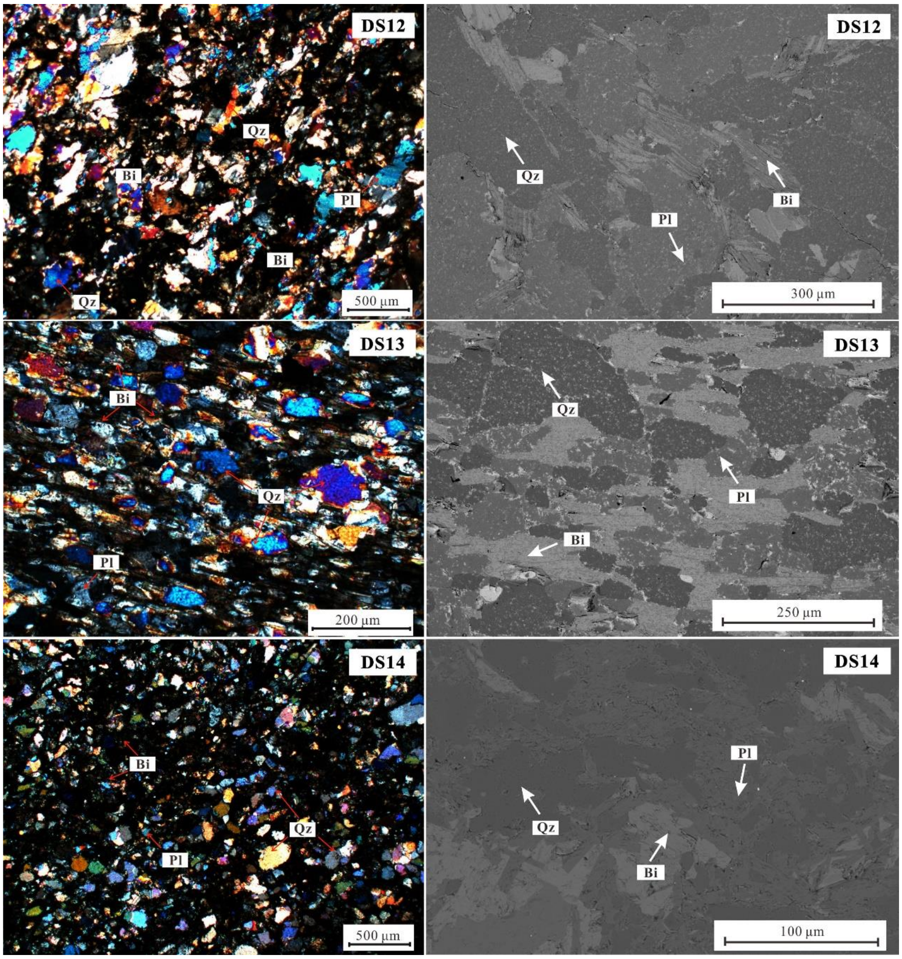
DS12
Qz
Bi
Pl
Bi
Qz
500 μm
DS12
Qz
Bi
Pl
300 μm
DS13
Bi
Qz
Pl
200 μm
DS13
Qz
Pl
Bi
250 μm
DS14
Bi
Qz
Pl
500 μm
DS14
Pl
Qz
Bi
100 μm

Fig. 2

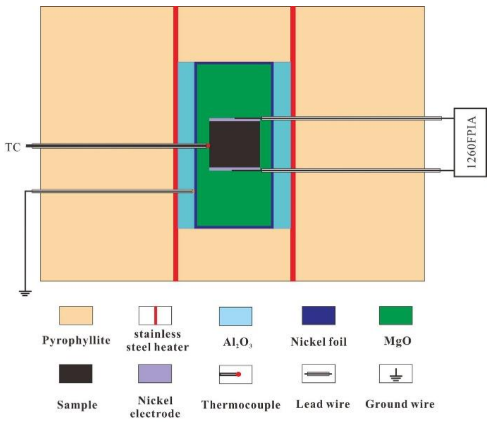
TC
1260FPIA
Pyrophyllite
stainless steel heater
Al_2O_3
Nickel foil
MgO
Sample
Nickel electrode
Thermocouple
Lead wire
Ground wire

Solid Earth Discuss., https://doi.org/10.5194/se-2017-103
Manuscript under review for journal Solid Earth
Discussion started: 27 September 2017

Fig. 3

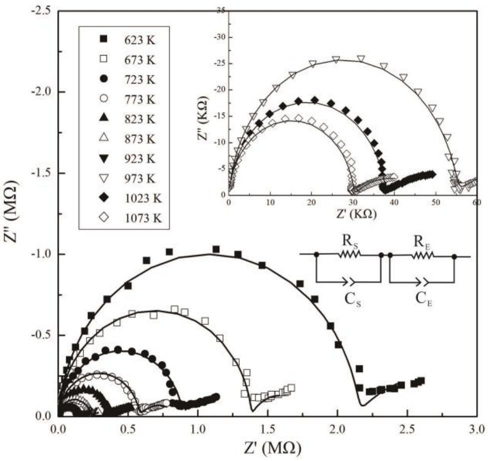

Fig. 4

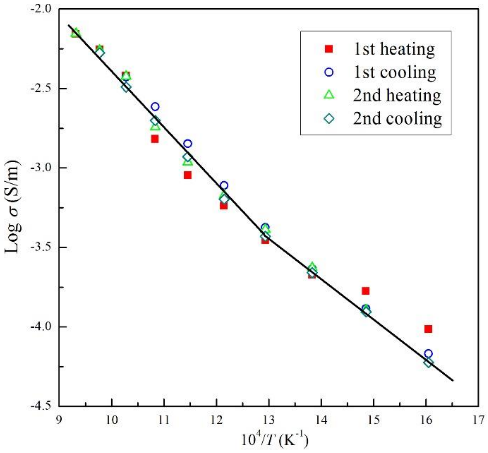
1st heating
1st cooling
2nd heating
2nd cooling
Log σ (S/m)
10⁴/T (K⁻¹)
-2.0
-2.5
-3.0
-3.5
-4.0
-4.5
9
10
11
12
13
14
15
16
17

Solid Earth Discuss., https://doi.org/10.5194/se-2017-103
Manuscript under review for journal Solid Earth
Discussion started: 27 September 2017

553 Fig. 5

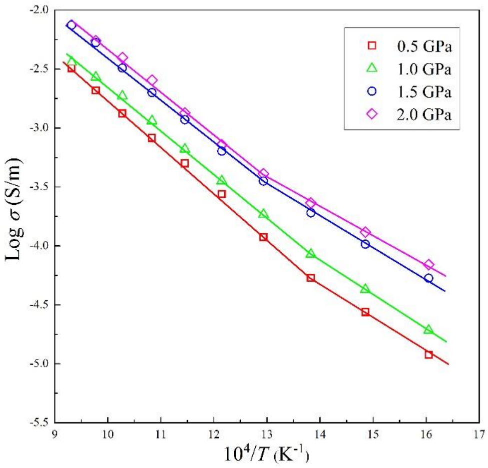

554

555

Fig. 6

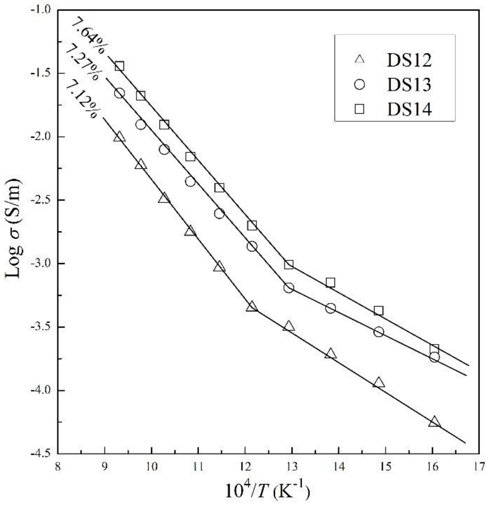

Solid Earth Discuss., https://doi.org/10.5194/se-2017-103
Manuscript under review for journal Solid Earth
Discussion started: 27 September 2017

Fig. 7

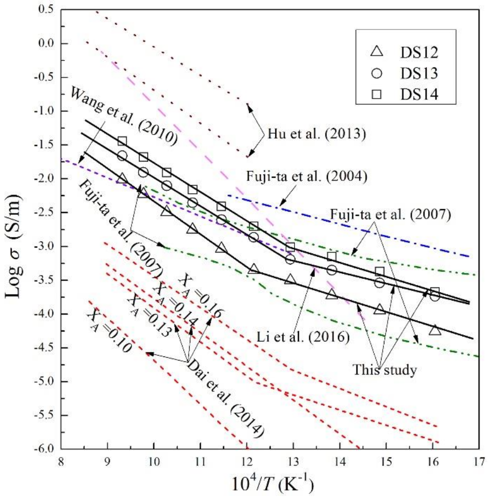

Solid Earth Discuss., https://doi.org/10.5194/se-2017-103
Manuscript under review for journal Solid Earth
Discussion started: 27 September 2017

562 Fig. 8

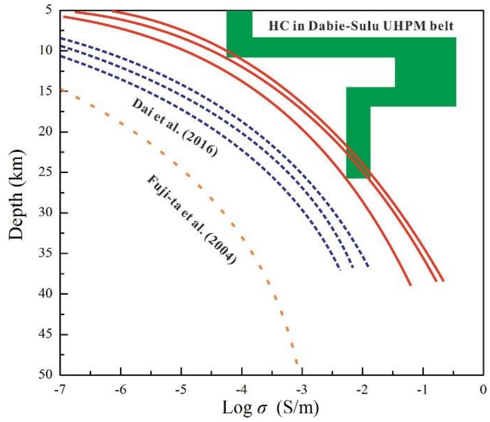

563